JAXA

JAXA Research and Development Report

Non-contact Thermophysical Property Measurements of Liquid and Supercooled Platinum

Takehiko ISHIKAWA, Paul-François PARADIS,
and Noriyuki KOIKE

January 2006

Japan Aerospace Exploration Agency

Non-contact Thermophysical Property Measurements of Liquid and Supercooled Platinum

By

Takehiko Ishikawa,[1] Paul-Francois Paradis,[1] and Noriyuki Koike[2]

Abstract : Thermophysical properties of equilibrium and supercooled liquid platinum were measured using non-contact diagnostic techniques with an electrostatic levitator. Over the 1691 to 2216 K temperature range, the density can be expressed as $\rho(T) = 19.2 \times 10^3 - 0.96 \ (T - T_m)$ (kg m^{-3}) with $T_m = 2041$ K, yielding a volume expansion coefficient of 5.0×10^{-5} K^{-1}. In addition, the surface tension can be expressed as $\gamma(T) = 1.80 \times 10^3 - 0.14 \ (T - T_m)$ (10^{-3}N m^{-1}) and the viscosity as $\eta(T) = 0.25 \exp [4.99 \times 10^4/(RT)]$ (10^{-3}Pas) over the 1743 to 2313 K temperature range.

KEY WORDS : platinum, liquid, density, surface tension, viscosity

1. Introduction

Platinum is a silver-white, malleable, and ductile metal. Because it does not oxidize in air at any temperature, platinum is widely used in jewelry, wire, and vessels for laboratory use, and in many valuable instruments including thermocouple elements. There is also much current interest in the use of platinum as a catalyst in fuel cells and in antipollution devices for automobiles.[1]

Knowledge of its thermophysical properties and their temperature dependence in the liquid state is important for studies on phase transformations, nucleation, atomic dynamics, and surface physics, as well as for industrial processes (e. g., refining, casting, and welding). These properties are also useful when designing alloys because the properties of component elements in the liquid state are required to estimate those of the final alloy (e.g., binary, ternary systems). However, because of its high melting point (2041 K),[2] and risk of contamination from the container wall, it is challenging to perform the measurement of thermophysical properties in its liquid state using conventional methods.

In this study, electrostatic levitation in vacuum overcame the contamination problems associated with the conventional high temperature processing and allowed accurate determination of the density, surface tension, and viscosity.[3,4] This paper first briefly describes the experimental facility and the measurement methods, and then presents the experimental results.

2. Experimental Setup and Procedures

2. 1. Electrostatic Levitation Furnace

The measurements were made using an electrostatic levitator (Fig. 1),[3,4] which consisted of a chamber evacuated to a

[1] Japan Aerospace Exploration Agency, 2-1-1 Sengen, Tsukuba, Ibaraki, Japan 305-8505.

[2] Chiba Institute of Technology, 2-17-1 Tsudanuma, Narashino, Chiba, Japan.

~10^{-5} Pa vacuum level before processing was initiated. The chamber housed a sample charged by electronic emission and levitated between electrodes via a feedback loop. The two disk electrodes were used for the vertical position control whereas four spherical electrodes were dedicated to horizontal control.[5] The positioning control relied on two sets of orthogonally arranged He–Ne lasers and the associated position detectors. The three dimensional sample position information was fed to a computer that generated and sent appropriate x, y, and z position control signals to high voltage amplifiers so that a prefixed sample position can be maintained. The lower electrode was surrounded by four coils that generated a rotating magnetic field that was used for rotation control.[6] Specimens were prepared by arc melting 99.8% mass purity platinum wire (Nilaco Corp., Japan) into spheroids with diameters of $ca.$ 1.5 mm.

Three laser beams were used for sample heating (Fig. 1). The beam of one CO_2 laser (10.6 μm emission) was sent directly to the sample whereas that from another CO_2 laser was divided into two beams such that the three focused beams in a same plane, separated by 120 degrees, hit the specimen. This configuration provided temperature homogeneity, sample position stability, and helped to control sample rotation.

The radiance temperature was measured with a single–color pyrometer (0.90 μm, 120 Hz acquisition rate) covering a 900 to 3800 K interval. The temperature was calibrated to true temperature using the melting plateau of the sample (T_m = 2041 K).

The sample was observed by three charge–coupled–device (CCD) cameras. One color camera offered a view of both the electrodes and the sample whereas two black and white high–resolution cameras (camera–1 and camera–2), located at right angles from each other and equipped with telephoto objectives, provided magnified views of the sample for density measurements. This also helped to monitor the sample position in the horizontal plane and to align the heating laser beams to minimize photon–induced horizontal sample movement and sample rotation.[7].
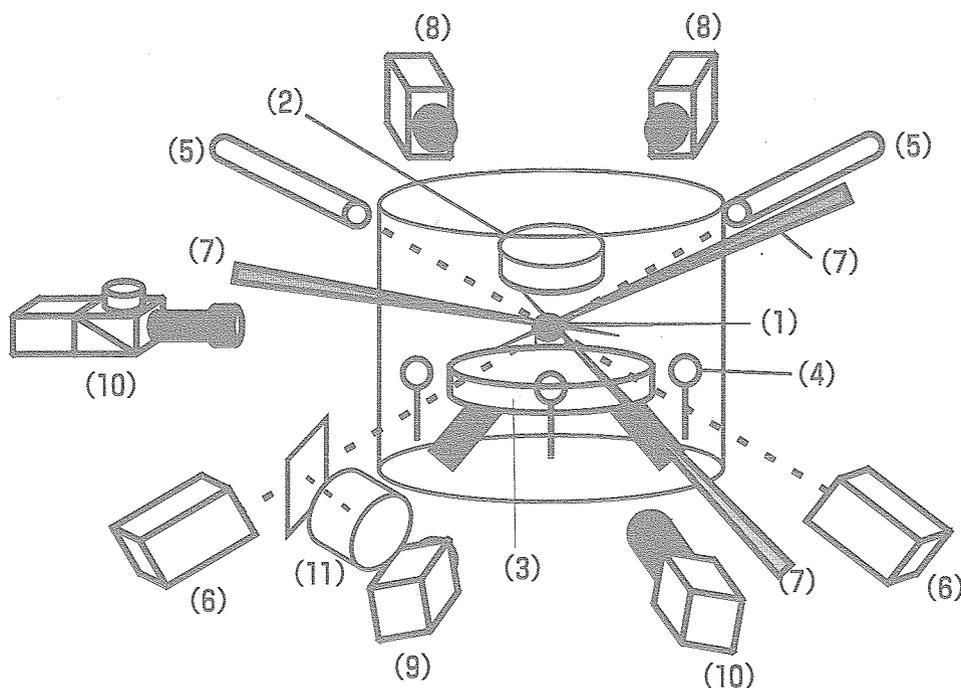

Fig. 1 Schematic view of the electrostatic levitation furnace and its diagnostic apparatus :
(1) sample, (2) top electrode, (3) bottom electrode, (4) side electrode, (5) He–Ne laser, (6) position detector, (7) CO_2 laser beam, (8) pyrometer, (9) CCD camera, (10) CCD camera with telephoto objective lens, (11) oscillation detector with a beam splitter.

2. 2. Thermophysical Properties Determination

Density measurements were carried out using a UV imaging technique described in detail elsewhere.[8,9] First, a solid sample was levitated and rotation about the vertical-axis was induced by a rotating magnetic field. The rotation rate of the solid sample was measured by a rotation detector, which monitors the intensity of He-Ne lasers reflected from the uneven sample surface.[6] When the rotation rate reached 10 Hz, the rotating magnetic field was turned off. All CO_2 laser beams were directed in such a way to minimize photon-induced rotation during the sample heating. Once a levitated sample was melted (ca. 1.5 mm diameter, nearly 30 mg), it became spherical due to surface tension and the distribution of surface charge. If the shape of a molten sample departed from that of a sphere (due to excessive rotation), a counter torque was applied by the magnetic field to restore the spherical shape. The controlled sample rotation not only improved the temperature homogeneity of the sample,[10] but also prevented precession and ensured the axi-symmetry of the sample along the vertical axis.
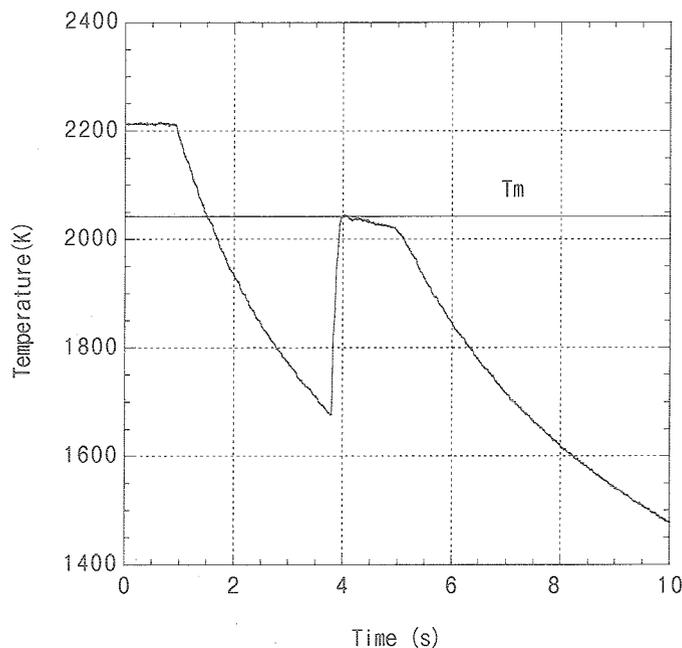

Fig. 2   Radiative temperature profile for a platinum sample showing supercooling and recalescence.

Images at the rate of 30 frames/s and temperature data were simultaneously recorded as a function of time. All laser beams were then blocked with mechanical shutters allowing the sample to cool radiatively. After the experiment, the video images from one high-resolution camera were digitized. Since the sample was axi-symmetric, the sample volume could be calculated from each image. The recorded images were calibrated by levitating a stainless sphere with a precisely known radius under identical experimental conditions. The images were then matched with the thermal history of the sample (Fig. 2). Because the mass of the sample was known, the density could be determined as a function of temperature. Although the sample evaporated as evidenced by a change in radius during long levitation periods (hours), the density experiments lasted only a few minutes, for which the melting temperature was exceeded for only a few seconds (Fig. 2). Therefore, the effect on density was negligible.

The surface tension and viscosity were determined by the oscillating drop method.[11] In this method, a solid sample was first levitated, rotated around 10 Hz, heated, melted, and brought to a selected temperature. Then, a $P_2(\cos\theta)$-mode drop oscillation was induced to the sample by superimposing a small sinusoidal electric field on the levitation field. One

4

of the positioning He–Ne laser beams was divided by a beam splitter and lead to a oscillation detector, which consisted of a power detector and a vertical slit. The shadow of the levitated sample was projected on this oscillation detector and fluctuation of the vertical diameter of the sample was translated to an electrical signal.[11] The transient signal that followed the termination of the excitation field was detected and analyzed using a custom–made program. This was done several times at a given temperature and repeated for several temperatures. Using the characteristic oscillation frequency ω_c of the signal, which was calculated by a fast Fourier transform (FFT) analysis and then corrected for non uniform surface charge distribution, the surface tension γ can be determined from :[12]

$$\omega_c^2 = \left(\frac{8\gamma}{\rho r_0^3} \right) Y, \tag{1}$$

where r_0 is the radius of the sample, ρ is the density, and Y is the correction factor that depends on the drop charge, the permittivity of vacuum, and the applied electric field.[13,14] Similarly, using the decay time τ given by the same signal, the viscosity η can be determined by

$$\eta = \frac{\rho r_0^2}{5\tau} . \text{ [15]} \tag{2}$$

During the experiments, the video images from a high–resolution camera were recorded. After the experiment, each value of the radius at each oscillation was obtained by image analysis. This procedure eliminated the measurement error due to sample evaporation. Moreover, the aspect ratio of the sample (ratio between the horizontal and vertical radii) was also calculated to evaluate the experimental error induced by sample rotation.

2. 3. Experimental Uncertainties

The experimental uncertainty for density measurements was derived from the respective uncertainty measurements for the mass and volume of samples. Because the uncertainty in mass was 0.1 mg while a typical platinum sample mass was 30 mg, the uncertainty can be estimated to be around 0.3 %. The uncertainty of volume ($\Delta V/V$) can be calculated by

$$\frac{\Delta V}{V} = \frac{3\Delta r_0}{r_0} \tag{3}$$

where Δr_0 is the uncertainty in radius measurement by the image analysis[9]. In our experiment, the average value of Δr_0 was around 1 pixel, while r_0 was 160 pixels. Therefore, $\Delta V/V$ can be estimated to be around 1.9 %, and the overall uncertainty of density measurement ($\Delta\rho/\rho$) was estimated to be about 2 %.

Based on equation (1), the uncertainty in surface tension measurement was mainly determined by those of ρ, r_0, and ω_c. As described earlier, the uncertainty of ρ and r_0 were 2 % and 0.65 %, respectively. The uncertainty of ω_c induced by the FFT analysis was negligibly small (0.4 %) by considering the transformation error (less than 1 Hz) and the typical characteristic oscillation frequency (around 250 Hz). As a result, the uncertainty of surface tension measurements ($\Delta\gamma/\gamma$) can be estimated to be around 3 % by the following equation :

$$\frac{\Delta\gamma}{\gamma} \approx \sqrt{ \left[\frac{\Delta\rho}{\rho} \right]^2 + \left[\frac{3\Delta r_0}{r_0} \right]^2 + \left[\frac{\Delta\omega_c}{\omega_c} \right]^2 } . \tag{4}$$

Similarly, the uncertainty of viscosity measurement can be estimated by the uncertainties of ρ, r_0, and τ. The uncertainty of the decay time $\Delta\tau$ was estimated to be about 15 %, which was due mainly to the sample motion with respect to the oscillation detector during drop oscillation. This determined the overall uncertainty of viscosity.

3. Results and Discussions

3. 1. Density

The density measurements of liquid platinum, taken over the 1691 to 2216 K temperature range and extending into the supercooled region by 350 K, are shown in Fig. 3. Several data points in Fig. 3 are shown with 2 % experimental error bars. The density, like that of other pure metals, exhibits a linear behavior as a function of temperature and can be fitted by the following relationship with a confidence interval of 95 % :

$$\rho(T) = (19.22 \pm 0.38) \times 10^3 - (0.96 \pm 0.01)(T - T_m) \text{ (kg m}^{-3}) \text{ (1691 to 2216 K)} \tag{5}$$

where T_m is the melting temperature (2041 K). The volume variation $V(T)$ of the molten state, normalized with the volume at the melting temperature V_m, was derived from Eq. (5), and can be expressed by

$$V(T)/V_m = 1 + 5.0 \times 10^{-5}(T - T_m) \tag{6}$$

where 5.0×10^{-5} (K^{-1}) represents the volume expansion coefficient.

Density data taken by other researchers are depicted in Fig.3 and listed in Table-I. As for the density at the melting temperature (ρm), our value agreed well with other reported values.[16-18]

The measured data for the temperature dependence of density were split to two groups. The first group, which contained the datum measured by Been et al. (−2.88 kg m^{-3} K^{-1}) with the maximum bubble pressure method and that obtained by Dubinin et al. (−2.4 kg m^{-3} K^{-1}) with the sessile drop method[16] showed very large values. On the other hand, the second group, which consisted of our result (−0.96 kg m^{-3} K^{-1}) and those of Hixson (−1.7 kg m^{-3} K^{-1}) and Gathers (−1.3 kg m^{-3} K^{-1}) determined with the pulse heating methods[17,18], exhibited measured values that were relatively small.

According to Morita and Guthrie,[19] the temperature dependence of density on transition metals (Fe, Co, Ni, and Pd) ranged from −0.9 to −1.2 kg m^{-3} K^{-1}. Our result was within this range, while the data of the first group were about 2.5 times larger. Table-II shows the temperature coefficients of density and thermal expansion coefficients of liquid transition

Table-I   Literature values for the density of platinum.

Density @ T_m (10^{3}kg m^{-3})	Temperature coefficient. (kg m^{-3} K^{-1})	Temperature (K)	Reference	Technique
19.2	−0.96	1691−2216	Present work	Levitation
19.7		2041	Eremenko[16]	Drop volume
18.82		2073	Kozakevitch[16]	Sessile drop
18.91	−2.882	2041−2148	Been[16]	Bubble pressure
18.81			Martsenyuk[16]	
19.77	−2.4	2041−2473	Dubinin[16]	Sessile drop
19.3	−1.7*	2041−5100	Hixson[17]	Pulse heating
19.1	−1.3**	2095−4500	Gathers[18]	Pulse heating

*Result of linear fitting between 2041 and 2750K

** Result of linear fitting between 2095 and 2690K

Table-II Thermal expansion coefficients of liquid metals measured by the electrostatic levitator.

Elements	Zr	Nb	Mo	Ru	Rh	Hf	Ta	W	Re	Ir	Pt
Density @ T_m (10^3kg m^{-3})	6.21	7.73	9.11	10.8	10.8	11.8	14.8	16.4	18.4	19.9	19.2
$-d\rho/dT$ (kg m^{-3} K^{-1})	0.27	0.39	0.60	0.56	0.76	0.55	0.82	1.08	0.91	0.71	0.96
Thermal expansion coefficient (10^{-5}K^{-1})	4.3	5.0	6.6	5.1	7.0	4.6	5.5	6.6	4.9	3.6	5.0

Data (except for Ta, W, and Re) were taken from Ref. 20.

Data of Ta were from Ref. 21.

Data of W were from Ref 22.
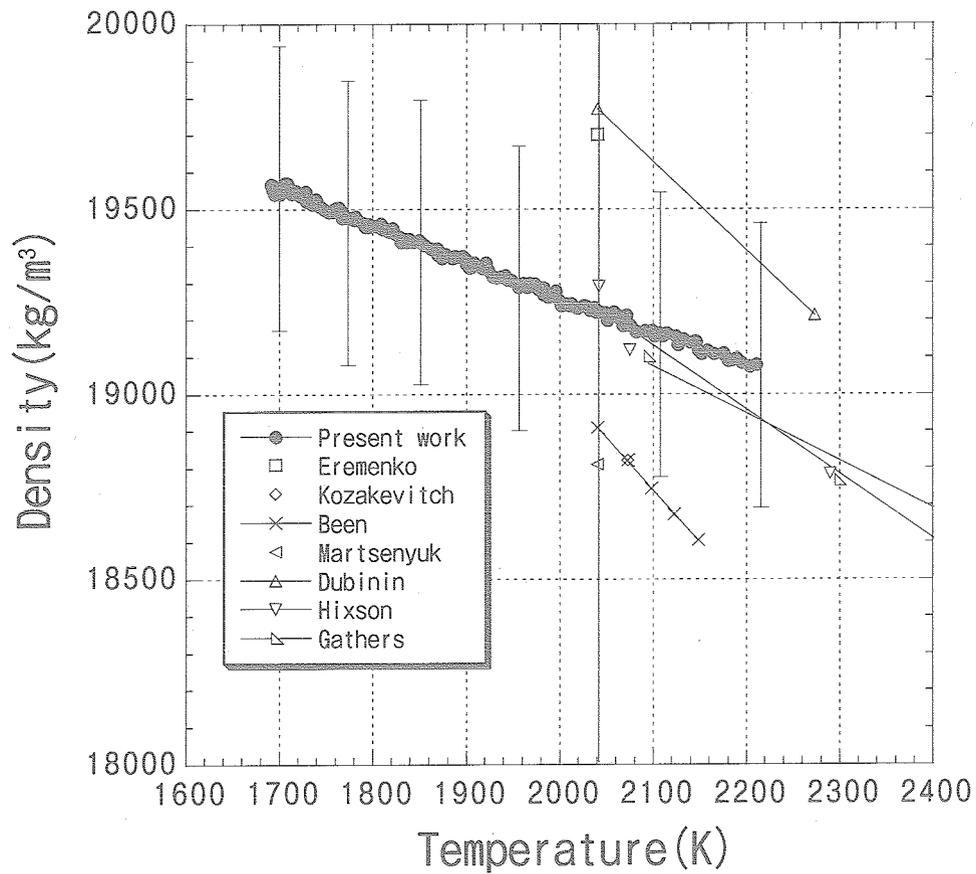
Fig. 3. Density of liquid platinum versus temperature.

metals measured by the electrostatic levitator. The thermal expansion coefficient of platinum was similar to those of other transition metals. In case of Been et al. and Dubinin et al., thermal expansion coefficients are 15.2 x 10^{-5} K^{-1} and 12.1 x 10^{-5} K^{-1} respectively, which are extremely large when compared with other transition metals.

Since the data of the first group were obtained with container techniques (whereas the second group used container-less techniques), it was suspected that the contamination from the crucibles could have affected the density measurements.

A simple relationship between the temperature dependence of the density of liquid metals and their boiling temperatures (T_b) was proposed by Steinberg[22]. He collected liquid density data at the melting point and the temperature dependence of liquid density for 44 elements and found the following empirical relations

$$-\frac{d\rho}{dT} \propto \frac{\rho_{00}}{T_b} \tag{7}$$

where ρ_{00} was the virtual density of the liquid at 0 K determined by extrapolation from ρ_m and T_m with :
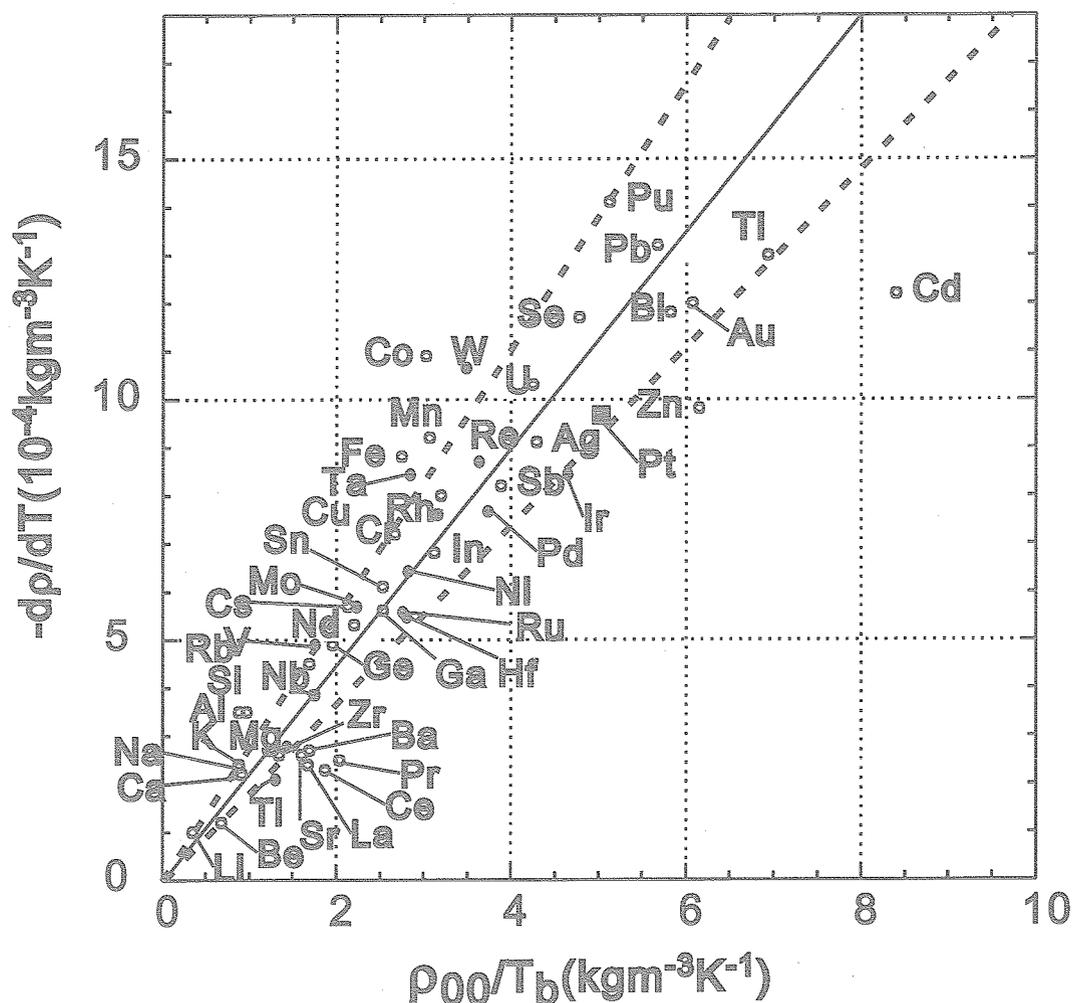
$$\rho_{00} = \rho_m - \frac{d\rho}{dT} T_m \tag{8}$$

Fig. 4. Correlation of $d\rho/dT$ with ρ_{00}/T_b for elements. Open and black circles represent data from Ref. 19 and refractory metals measured by electrostatic levitator, respectively. Pt points in Ref. 23 fall outside the range of figure (its ordinate is 28.8 and its abscissas is 6.05). Pt data in present work is plotted with black square. The solid line is the best fit to data and the dashed lines represent the 20% error cone from Ref.23.

Figure 4 illustrates the correlation of $-d\rho/dT$ with ρ_{00}/T_b. In his study, Most of metal elements followed the correlation except for mercury and platinum. In Fig.4, our measured data of refractory metals including that of platinum were also plotted. Our platinum data (-0.96 kg m^{-3} K^{-1}), as well as those for other refractory metals, showed a good agreement with the Steinberg's relation.

3. 2. Surface Tension

Figure 5 depicts the results for the surface tension of platinum. Several data points in Fig. 5 are accompanied with 3 % error bars to indicate the experimental uncertainty described in 2.3. Data available from the literature were superimposed on the same figure for comparison and listed in Table-III. The surface tension data, measured over the 1743 to 2313 K temperature range and extending into the supercooled region by 298 K, can be expressed with a confidence interval of 95 % by

$$\gamma(T) = (1.80 \pm 0.05) \times 10^3 - (0.14 \pm 0.01) \ (T - T_m) \ (10^{-3} \text{N m}^{-1}) \ (1743 \text{ to } 2313 \text{ K}). \qquad (9)$$

Around the melting temperature, except for the value measured by Quincke with the capillary rise method,[23] the discrepancy between the datum of the present work and those in the literature was within ±5%, which constitutes a good agreement considering the experimental uncertainty of each measurement. However, the data measured by the capillary rise method and the sessile drop method, both of which used a container or substrates, tended to show lower values. The cause could be sample contamination from the walls.

Our measured value of the temperature dependence of the surface tension (-0.14×10^{-3} N m^{-1} K^{-1}) was 2.2 times smaller than that reported by Dubinin (-0.307×10^{-3} N m^{-1} K^{-1}).[23] This discrepancy could be explained by the following two reasons. At first, just like equation (1), every formula for each surface tension measurement method used the density data. Usually the surface tension is proportional to the density. Dubinin et al. have most likely used the density value of their own measurement, whose temperature coefficient was 2.5 times larger than that of present work, as shown in Table-I. The second reason was the difference in temperature range. Our measurement covered an interval of 570 K, while Dubinin el al. obtained data only over a 107 K temperature range. Data with a wider temperature range offered a more accurate temperature dependence. Our value was very close to that estimated by Allen (-0.17×10^{-3} N m^{-1} K^{-1})[28] with the following equation ;

$$\frac{d\gamma}{dT} = \frac{\gamma}{T_c - T} \left[\frac{2 \ (T_c - T)}{3\rho} \frac{d\rho}{dT} - 1 \right] \qquad (10)$$

where T_c is the critical temperature.

Kasama et al.[29] proposed an empirical equation based on a physical model. Based on this model, surface tension and its temperature dependence can be expressed as

$$\gamma = \frac{1}{2} \frac{\pi^2 C^2 \delta^2 T_m}{N_A \ M^{2/3}} \left(\frac{\rho}{\rho_m} \right)^{2/3} \{(\alpha+1) \ \rho^{1/3} - \rho_m^{1/3}\}^2 \qquad (11)$$

$$\frac{d\gamma}{dT} = -\frac{1}{3} \frac{\pi^2 C^2}{N_A} \frac{T_m \ \Lambda \delta^2}{M^{2/3}} \{2 \ (\alpha+1)^2 \ \rho^{1/3} \rho_m^{2/3} + \rho^{-1/3} - 3 \ (1+\alpha) \ \rho_m^{-1/3}\}$$

where N_A was Avogadro's number, M was atomic number, Λ was the temperature dependence of density ($-d\rho/dT$), respectively. A constant C was derived from Lindemann's theory of melting and ranged from 2.8×10^{12} to 3.1×10^{12}, d was a ratio between the characteristic vibration frequency in the liquid phase and solid phase and estimated around 0.5, and α was a constant to determine the distance where an attractive force by an atom was effective and ranged 0.45 to 0.65, respectively.

Table-III   Literature values for the surface tension of platinum.

Surface Tension @ T_m $(10^{-3} N\ m^{-1})$	Temperature coefficient. $(10^{-3} N\ m^{-1}\ K^{-1})$	Temperature (K)	Reference	Technique
1800	−0.14	1743−2313	Present work	Levitation
1869		2041	Quincke[24]	Drop weight
1673		2053	Quincke[24]	Capillary
1740		2041	Eremenko[24]	Drop weight
1699		2073	Kozakevitch[24]	Sessile drop
1800		2041	Allen[25]	Pendant drop
1746	−0.307	2041−2148	Dubinin[24]	Sessile drop
1865		2041	Kingery[26]	Pendant drop
1707		2043	Martsenyuk[27]	
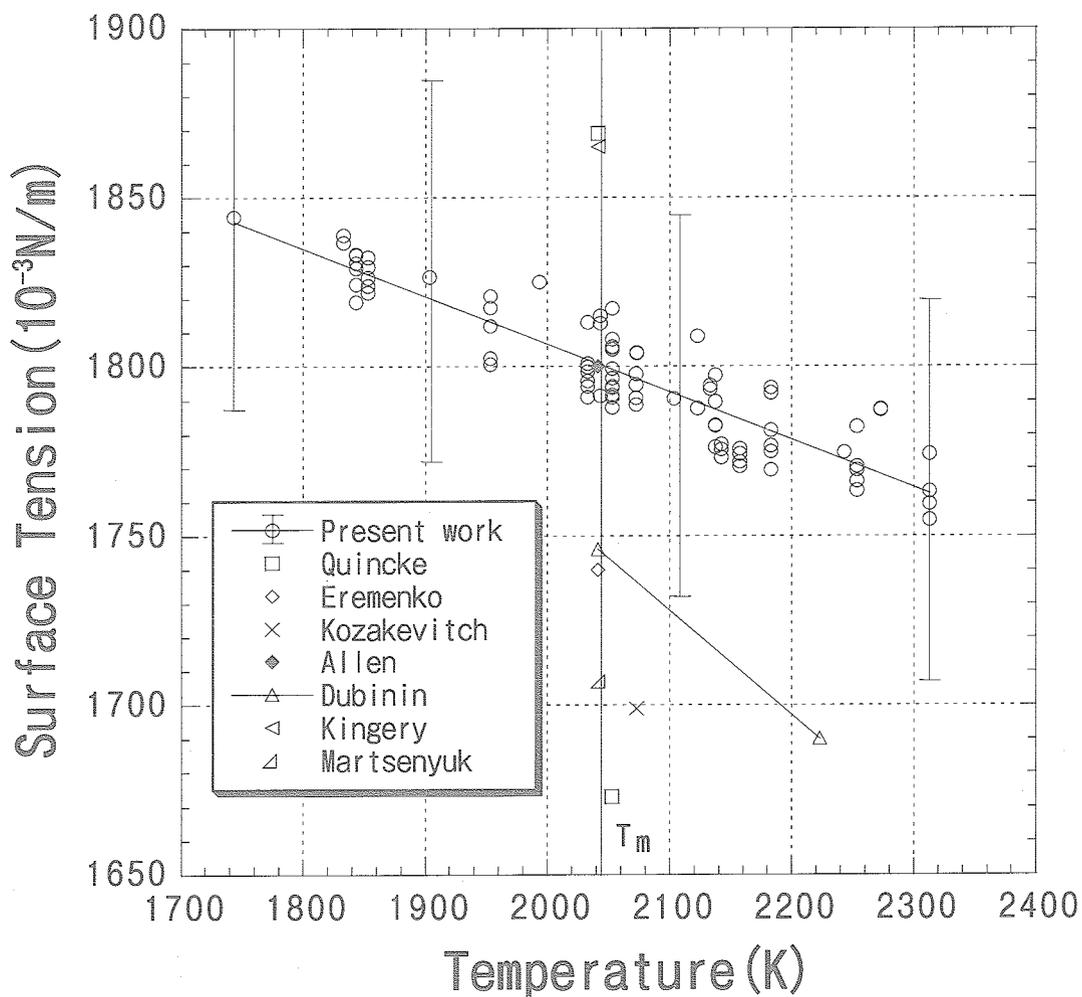
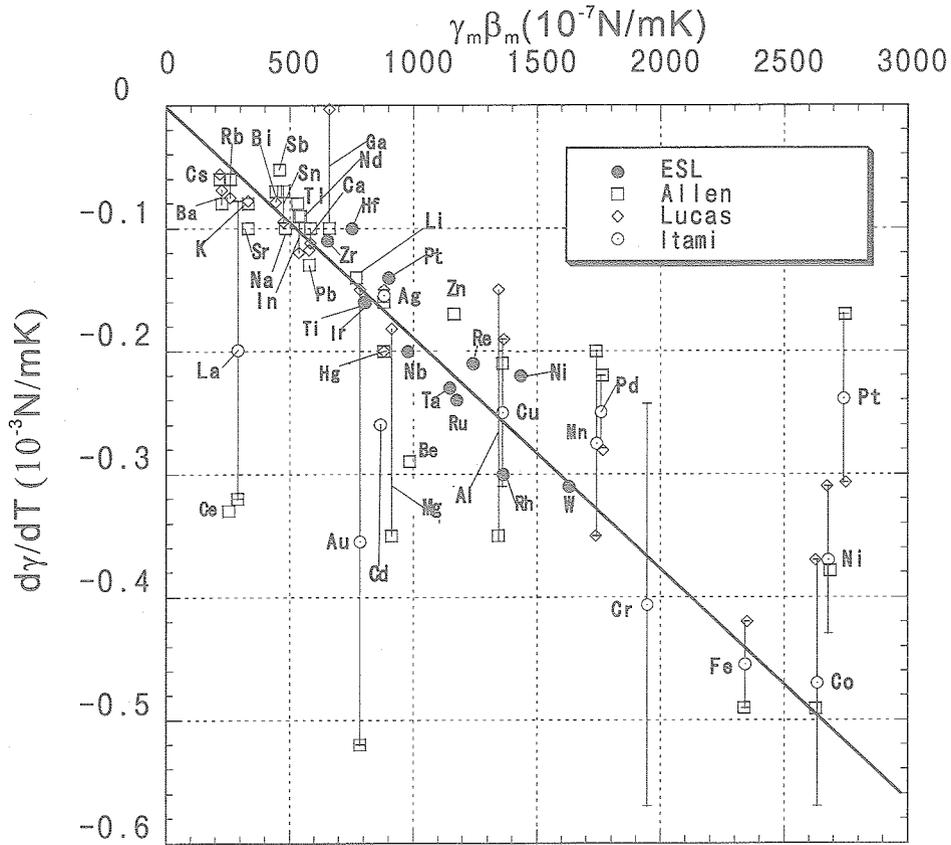Fig. 5.   Surface tension of platinum versus temperature.

Fig. 6 Correlation between $\gamma_m \beta_m$ and $d\gamma/dT$

At the melting temperature, the temperature coefficient of the surface tension could be calculated by

$$\frac{d\gamma}{dT} = -\frac{1}{3} \frac{\pi^2 C^2}{N_A} \frac{T_m \Lambda \delta^2}{M^{2/3}} \rho_m^{-1/3} (2\alpha^2 + \alpha) \qquad (12)$$

In this formula, uncertainty of those constants (C, α, and d) seriously affected the temperature dependence of surface tension. Two of those constants could be eliminated by combining the equations (11) and (12), and the temperature coefficient of the surface tension could be determined as

$$\frac{d\gamma}{dT} = -\frac{2}{3} \frac{\Lambda \gamma_m}{\rho_m} \frac{2\alpha+1}{\alpha} = K \frac{\Lambda \gamma_m}{\rho_m} = K \gamma_m \beta_m \qquad (13)$$

$$K \equiv \frac{-2 (2\alpha+1)}{3\alpha}$$

and this equation suggested that the temperature dependence of surface tension was proportional to the multiple of surface tension at melting temperature and thermal expansion coefficient.

Validity of this formula for liquid metals was checked by using literature datum[28,30,31] and our measurements with the electrostatic levitator (ESL)[32]. Results are shown in figure 6.

Literature data of alkaline metals showed good agreements with the equation (13), while those of transition metals scattered and some of them were far from the relation. On the other hand, measured data of refractory metals with ESL showed same tendency as the alkaline metals. Particularly, platinum and nickel data by our measurement followed the relation, while those of reference didn't. Based on the results with the ESL, temperature dependence of surface tension of metal elements could be estimated if surface tension at their melting temperature and thermal expansion coefficient were

known.

Temperature dependence of surface tension is an important parameter to evaluate the magnitude of the thermo-capillary flow when the floating zone method or Czochralski method are used for single crystal growth of semiconductors. Based on our result, particular attention should be paid to the temperature dependence of density when the temperature dependence of surface tension are discussed.

3. 3. Viscosity

Figure 7 illustrates our data that can be fitted by the following Arrhenius function :

$$\eta(T) = 0.25\exp\left[4.99 \times 10^4 \ /(RT)\right] \ (10^{-3}\text{Pa s}) \ (1743 \text{ to } 2313 \text{ K}), \qquad (14)$$

where R, the gas constant, is equal to 8.31 J mol^{-1} K^{-1}. The scatter observed in the data is mainly due to the motion of the sample with respect to the oscillation detector. Literature values are also listed in Table-IV and plotted in Fig.7. Our

Table-IV   Literature values for the viscosity of platinum.

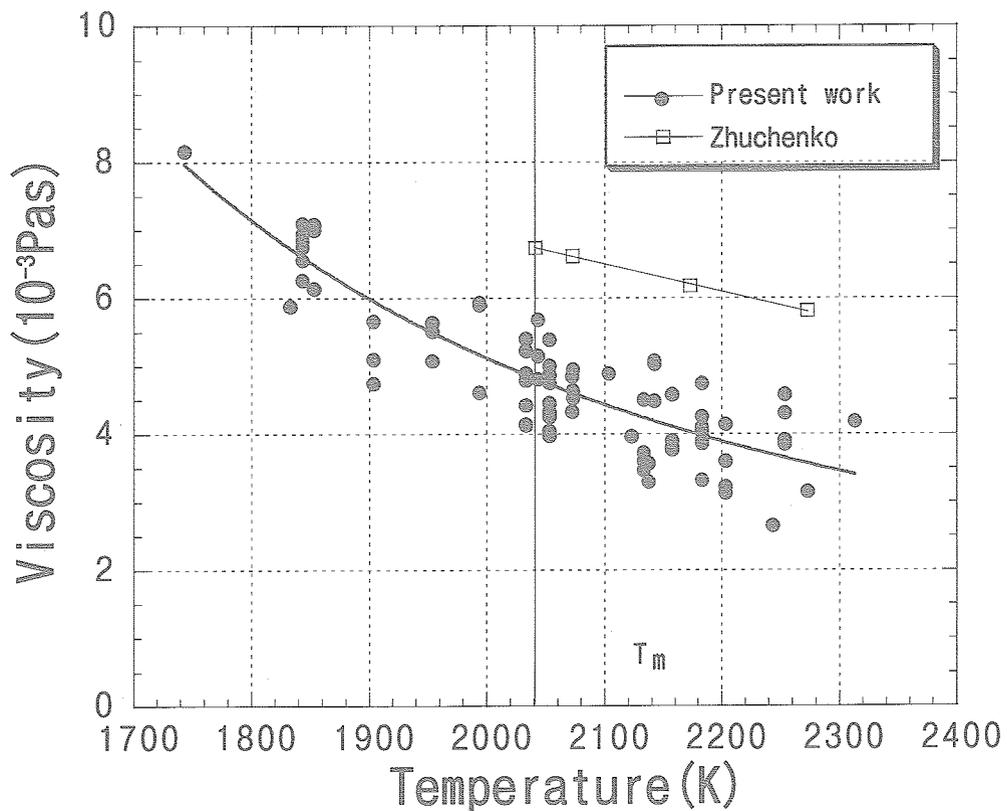| Viscosity @ T_m (10^{-3}Pa s)	$\eta(T) = \eta_0\exp(E_0/RT)$		Temperature (K)	Reference	Technique
	η_0 (10^{-3}Pa s)	E_0 (kJ mol^{-1})			
4.82	0.25	49.9	1743–2313	Present work	Levitation
6.74	1.53	25.263	2041–2273	Zhuchenko[29]	

Fig. 7.   Viscosity of platinum versus temperature.

measured viscosity at the melting temperature (4.8 x 10^{-3} Pa s) was 30% smaller than that of Zhuchenko[33]. Compared with density or surface tension, the measured data for viscosity are very scarce. Additional data are necessary to determine the recommended value for the viscosity of platinum.

4. Conclusions

The density, the surface tension, and the viscosity of liquid platinum were measured with an electrostatic levitator and the data were reported. The containerless processing and non–contact measurement techniques eliminated contamination from the crucibles as well as suppressed nucleation at the melting temperature. Those effect enabled the measurement of thermophysical properties over wide temperature ranges, including the supercooled state. Measurements with wider temperature range could determine the temperature dependence of each properties with higher accuracies. Our results of the temperature dependence of density and surface tension agreed well with the empirical equations provided by Steinberg and Allen.

Acknowledgments

Special thanks to Mr. S. Fukuyama (A. E. S. Co. ltd.) and Ms. A. Ishikura (Gakushuin University) for help in some experiments.

REFERENCES

1. D. R. Lide and H. P. R. Frederikse : *CRC Handbook of Chemistry and Physics,* (CRC Press, Boca Raton, Florida, 1997) 78th ed.
2. R. E. Bedford, G. Bonnier, H. Maas, and F. Pavese : Metrologia 33 (1996) 133.
3. P. –F. Paradis, T. Ishikawa, and S. Yoda : ESA SP–454 (2001) 993.
4. T. Ishikawa, P. –F. Paradis, and S. Yoda, J. Jpn. Soc. Microg. Appl. 18 106 (2001).
5. W. –K. Rhim, S. –K. Chung, D. Barber, K. –F. Man, G. Gutt, A. A. Rulison, and R. E. Spjut : Rev. Sci. Instrum. 64 (1993) 2961.
6. W. –K. Rhim and T. Ishikawa : Rev. Sci. Instrum. 69 (1998) 3628.
7. W. –K. Rhim and P. –F. Paradis : Rev. Sci. Instrum. 70 (1999) 4652.
8. T. Ishikawa, P. –F. Paradis, and S. Yoda : Rev. Sci. Instrum. 72 (2001) 2490.
9. S. –K. Chung, D. B. Thiessen, and W. –K. Rhim : Rev. Sci. Instrum. 67 (1996) 3175.
10. R. W. Hyers, D.M.Matson, K.F.Kelton, and J.R.Rogers : *Proc. Microgravity Transport Processes in Fluid, Thermal, Biological and Materials Sciences III,* Davos, Switzerland (2003).
11. Lord Rayleigh : Proc. R. Soc. London 29 (1879) 71.
12. W. –K. Rhim, K. Ohsaka, and P. –F. Paradis : Rev. Sci. Instrum. 70 (1999) 2996.
13. Lord Rayleigh : Philos. Mag. 14 (1882) 184.
14. J. Q. Feng and K. V. Beard : Proc. R. Soc. London A 430 (1990) 133.
15. H. Lamb : Hydrodynamics, (Cambridge University Press, 1932), 6th ed. 473.
16. G. Lang : CRC *Handbook of Chemistry and Physics*, ed. D. R. Lide, (CRC Press, Boca Raton, 1991–1992), 72nd ed. 4–124.
17. R. S. Hixson and M. A. Winkler : Int. J. Thermophysics, 14 (1993) 409.
18. G. R. Gathers, J. W. Shaner, and W. M. Hodgson : High Temp. –High Press. 11 (1979) 529.
19. T. Iida and R. I. L. Guthrie : The Physical Properties of Liquid Metals, (Clarendon Press, Oxford 1988), 71.

20. T. Ishikawa, P. –F. Paradis, T. Itami, and S. Yoda : Measurement Science and Technology, 16 (2005) 443.

21. T.Ishikawa and P. –F. Paradis : in press, Journal of Electronic Materials.

22. P. –F. Paradis, T. Ishikawa, R. Fujii, and S. Yoda : Appl. Phys. Lett. 86 (2005) 41901.

23. D. J. Steinberg : Metallurgical Transactions 5 (1974) 1341.

24. G. Lang : *CRC Handbook of Chemistry and Physics,* ed. D. R. Lide, (CRC Press, Boca Raton, 1991–1992), 72nd ed. 4–133.

25. B. C. Allen, Trans. AIME 227 : 1175 (1963).

26. W. D. Kingery, Am. Ceram. Soc. Bull., 1956, 35, 108 : thorough International materials Reviews, 38 (1993), 157.

27. P.S. Martsenyuk, Inst. Tekh. Probl. Mater. Akad. Nauk SSSR, 1980,51–57 : through International materials Reviews,38 (1993), 157.

28. B. C. Allen : *Liquid Metals Chemistry and Physics,* ed. S. Z. Beer (Marcel Dekker, 1972), Chap. 4, 188.

29. A. Kasama, T. Iida, and Z. Morita, *J. Japan Inst. Metals,* 40 (1976), 1030.

30. L. D. Lucas, *Tech l'Ing.,* 7, Form. M65 (1984).

31. T. Itami, in *Condensed Matter Disordered Solids*, ed. S. K. Srivastava and N. H. March (World Scientific. 1995), Chap.3.

32. T. Ishikawa, P. –F. Paradis, T. Itami, and S. Yoda, *JAXA Research and Development Report,* JAXA–RR–04–024E (2005).

33. A. A.Zhuchenko, E. L. Dubinin, A. I. Timofeev, and S. O. Safonov, Izv. Vyssh. Uchebn. Zaved. Tsvetn. Metall. 4 (1977), 142 : thorough *Condensed Matter Disordered Solids*, ed. S. K. Srivastava and N. H. March (World Scientific. 1995), Chap.3, p.232.

JAXA

Japan Aerospace Exploration Agency